Published in final edited form as:
Cell Signal. 2013 October ; 25(10): 2047–2059. doi:10.1016/j.cellsig.2013.05.012.

Fbxl12 triggers G1 arrest by mediating degradation of calmodulin kinase I

Rama K. Mallampalli[*,=], **Leah Kaercher**[*], **Courtney Snavely**[*], **Roopa Pulijala**[*], **Bill B. Chen**[*], **Tiffany Coon**[*], **Jing Zhao**[*], and **Marianna Agassandian**[*]

[*]Departments of Medicine, Acute Lung Injury Center of Excellence, the University of Pittsburgh, Pittsburgh, PA 15213 USA

[=]Department of Cell Biology and Physiology, The University of Pittsburgh, Pittsburgh, PA 15213 USA

[=]Medical Specialty Service Line, Veterans Affairs Pittsburgh Healthcare System

Abstract

Cell cycle progression through its regulatory control by changes in intracellular Ca^{2+} levels at the G1/S transition mediates cellular proliferation and viability. Ca^{2+}/CaM-dependent kinase 1 (CaMKI) appears critical in regulating the assembly of the cyclin D1/cdk4 complex essential for G1 progression, but how this occurs is unknown. Cyclin D1/cdk4 assembly in the early G1 phase is also regulated via binding to p27. Here, we show that a ubiquitin E3 ligase component, F-box protein Fbxl12, mediates CaMKI degradation via a proteasome-directed pathway leading to disruption of cyclin D1/cdk4 complex assembly and resultant G1 arrest in lung epithelia. We also demonstrate that i) CaMKI phosphorylates p27 at Thr^{157} and Thr^{198} in human cells and at Thr^{170} and Thr^{197} in mouse cells to modulate its subcellular localization; ii) Fbxl12-induced CaMKI degradation attenuates p27 phosphorylation at these sites in early G1 and iii) activation of CaMKI during G1 transition followed by p27 phosphorylation appears to be upstream to other p27 phosphorylation events, an effect abrogated by Fbxl12 overexpression. Lastly, known inducers of G1 arrest significantly increase Fbxl12 levels in cells. Thus, Fbxl12 may be a previously uncharacterized, functional growth inhibitor regulating cell cycle progression that might be used for mechanism-based therapy.

1. Introduction

During cell replication, the G1 phase is critical and regulated by integration of a variety of signals that determine whether the cell is destined to proliferate, differentiate, or die [1]. Thus, G1 progression and transition to the next phase is most essential in cell fate. The control of factors that mediate G1 phase transition are regulated partly by the Skp-cullin-F box (SCF) ubiquitin-ligase complexes that typically bind to phosphorylated substrates to mediate their ubiquitination and degradation [2]. F-box proteins contain two domains: an

Address Correspondence to: Marianna Agassandian, Ph.D, The University of Pittsburgh, Pulmonary, Allergy & Critical Care Medicine, BST 1, W1200-5B, 200 Lothrop St., Pittsburgh, PA 15213, Phone: (412) 383-7249, Fax: (412) 692-2260, agassandianm@upmc.edu.

Conflict of interest statement
All co-authors declare ***no conflict of interest*** for this publication.

NH_2-terminal F-box motif and carboxyl-terminal leucine-rich repeat (LRR) motif or WD repeat motif. The F-box motif binds Skip1, whereas LRR/WD are used for substrate recognition. The SCF complexes have emerged as important modulators of cell cycle progression in normal, transformed, or malignant cells via degradation of key regulatory proteins such as G1-phase cyclins, cyclin dependent kinase (cdk) inhibitors, transcription factors and others. In this SCF complex, the F box protein confers substrate recognition specificity. Recently, the F-box protein, Fbxo31, was shown to initiate G1 arrest via cyclin D1 degradation after DNA damage caused by γ-irradiation [3]. Another related protein, Fbxl12, mediates osteoblast cell differentiation by mediating $p57^{kip2}$ ubiquitin-proteasome degradation [4]. Unlike other SCF F- box proteins that usually target phosphodegrons, the recently described Fbxl2 protein targets cyclin D2 [5] or cyclin D3 [6] via recognition of a canonical calmodulin (CaM)-binding motif that induces Go or G2/M arrest respectively.

Calcium (Ca^{2+}) is a second messenger that is universally required for cell proliferation that via its ubiquitous intracellular receptor, CaM, activates calcium/calmodulin-dependent protein kinase (CaMK) cascades required for cell cycle transition. Eukaryotic cells are extremely sensitive to changes in intra and extracellular levels of calcium. For example, the lowering of extracellular Ca^{2+} decreases the rate of cell proliferation and causes G1 arrest where early G1 and G1/S checkpoints are the most sensitive to Ca^{2+} depletion during cell cycle progression [7,8]. The intracellular Ca^{2+} pool is also important as depletion of Ca^{2+} from intracellular stores induces accumulation of cells in a quiescent state [9].

Ca^{2+}/CaM-dependent kinases that comprise the CaMK family are involved in every stage of the cell cycle and are especially important for cell cycle entry and G1/S transition [10]. The activation of Ca^{2+}/CaM-dependent kinase 1 (CaMKI) belonging to this family is dependent on Ca^{2+}/CaM binding and phosphorylation by the upstream Ca^{2+}/CaM-dependent kinase kinase (CaMKK) for maximal activity [11,12,13]. Pharmacological inhibition of CaMKI/II induces G1 arrest in a variety of cell types via regulation of cyclin D1 expression, phosphorylation of the retinoblastoma protein (Rb), and by prevention of cdk4 activation or by increasing p27 association with cyclin dependent kinase 2 (cdk2) [14,15,16,17]. Recent studies using KN-93, a CaMKI/II inhibitor, demonstrates that CaMKI regulates cyclin D1/cyclin-dependent kinase 4 (cdk4) complex assembly via an unknown mechanism [18]. Cyclin D1/cdk4 assembly with p21/p27 results in an inactive complex that accumulates in the nucleus after KN-93-induced G1 arrest [18]. $p27^{Kip1}$ is a cyclin-dependent kinase 4 inhibitor that also facilitates assembly and activation of cyclin D-cdk(s) complexes in early G1 [19]. Hence, both p27 activity and its subcellular localization are critical in regulating G1 phase transition.

The activity of p27 is controlled by its phosphorylation state, subcellular localization, and its cellular concentrations and binding to different cell-cycle regulated complexes [20,21,22,23]. For normal cell cycle progression induced by mitogens, translocation of p27 from the nucleus to the cytoplasm in G0/early G1 is necessary. This nuclear export is mediated by the exportin (CRM1) and requires phosphorylation of p27 at serine 10 (S10) that can be achieved by actions of human kinase-interacting stathmin or by the serine/threonine kinases AKT, or CaMKII [23,24,25,26,27]. Phosphorylation of p27 at threonine 157 (T157) by AKT prevents its association with importin α and nuclear re-entry during G1 [28]. The other site, threonine 198 (T198) within p27 which promotes binding to 14-3-3 to facilitate p27 cytoplasmic localization is phosphorylated by AKT as well [23]. Recent studies have demonstrated that phosphorylation of p27 at T157 and T198 by PKB/AKT regulates assembly and activation of the cyclin D1/cdk4 complex in early G1 [29], whereas phosphorylation at Thr-187 (T187) leads to proteasomal degradation that can also occur via direct binding to a ubiquitin E3 ligase independently of T187 phosphorylation [30,31,32]. The binding of p27 to cyclin D1/cdk4 via phosphorylation within the p27 cdk interaction

domain at tyrosine residues also regulates its molecular behavior [33]. In addition, p27 can serve as a barometer of cellular deregulation of intracellular signaling and potential predictor of response to targeted therapies [34]. Thus, p27 is a major regulator of cell cycle progression that via its reversible phosphorylation modulates cyclin D1/cdk4 complex formation in early G1. CaMKI also controls cyclin D1/cdk4 complex assembly, however whether CaMKI exerts its regulatory control of G1 transition through p27 has not been elucidated.

Here, we demonstrate that the F box protein Fbxl12 mediates CaMKI proteasomal degradation that causes G1 arrest in lung epithelial cells. Fbxl12 reduces levels of cyclin D1 in the cyclin D1/cdk4 complex by indirectly modulating a new substrate for CaMKI, p27 that is integrally required for cyclin D1/cdk4 complex assembly. CaMKI phosphorylates human p27 at T157 and T198 and mouse p27 at T170 and T197 to regulate their subcellular localization. Thus, these data suggest that Fbxl12 is an endogenous CaMKI inhibitor that restricts cellular proliferation by modulating p27directed cyclin D1/cdk4 complex assembly.

2. Materials and Methods

2.1. Materials

MLE and A549 cell lines were obtained from the American Type Culture Collection (Manassas, VA). Recombinant CaMKI were from Millipore (Dundee, UK) and Abnova (Taipei City, Taiwan). The TnT reticulocyte assay system was from Promega (Madison, WI). Talon metal affinity resin was obtained from Clontech Laboratoties (Valencia, CA). The Quikchange Site-Direct Mutagenesis kit was from Stratagen (La Jolla, Ca). FuGENE 6 transfection reagent was purchased from Roche Diagnostic (Indianapolis, IN). CaMKI and pCaMKI antibody, *Fbxl12* siRNA, *CaMKI* si RNA and ubiquitin aldehyde were from Santa Cruz Biotechnology (Santa Cruz, CA). The p27, cdk4, cdk2, cyclin D1, cyclin E, Akt, pAkt (T308, S473), ubiquitin (P4D1) and anti-GST Alexa Fluor 647-conjugated antibodies were purchase from Cell Signaling (Danvers, MA). Fbxl12 recombinant protein and Fbxl12 antibody were obtained from Novus Biologicals (Littleton, CO). Anti-Penta-His Alexa Fluor-conjugated antibody was from QIAGEN (Valencia, CA). The phosphor-p27/kip1 (T198) antibody was purchased from R&D systems (Minneapolis, MN). Ubiquitin was from Enzo (Farmingdale, NY). The V5 antibody was obtained from Invitrogen (Carlsbad, CA). Anti-p27 KIP 1 (phosphor S10), anti-p27 KIP 1 (phosphor T157) antibody, p27 KIP1 GST-tagged protein and active form of CaMKI were purchased from Abcam (Cambridge, MA). *CaMKI* shRNA was from OriGene (Rockville, MD). Myc Tag Antibody was obtained from Aviva Systems Biology (San Diego, CA). The cell cycle phase determination kit was obtained from Cayman (Ann Arbor, MI). The *GFP-conjugated p27* plasmid (mouse) (15192) was purchased from Addgene (Cambridge, MA). *Pc DNA3 myc3* p27 (human) plasmid was obtained from Addgene (Cambridge, MA). The *Flag-p27*, *Flag-27T170A*, *Flag-27T197A* and *Flag-p27T170A/T197A* plasmids were a kind gift from Cheryl Lyn Walker (Department of Carcinogenesis, University of Texas M.D. Anderson Cancer Center, Huston). Rabbit igG TrueBlot kit was purchased from eBioscience (San Diego, Ca, USA). Super Signal west Femto kit was obtained from Thermo Scientific (Rockford, IL, USA). [γ ^{32}-P]-ATP was from Perkin Elmer Life Science (Waltham, MA, USA). KN-93, MG132 and cycloheximide inhibitors were purchased from Sigma-Aldrich (St. Louis, MO, USA).

2.2. Cell Culture

MLE cells were maintained in Hite's medium with 10% fetal bovine serum at 37°C. After reaching 80% confluence, the cells were harvested using trypsin and plated onto 6-well or 100-mm tissue culture dishes. In some experiments cells were starved by depletion of serum during 24–48 h or exposed to inhibitors. Cell lysates were prepared by brief sonication in

150 mM NaCl, 50 mM Tris, 1.0 mM EDTA, 2 mM dithiothreitol, 0.025% sodium azide and 1 mM phenylmethylsulfonyl fluoride (pH 7.4) at 4°C.

2.3. Immunoblot analysis

Equal amounts of proteins in sample buffer were resolved on SDS-10% PAGE, transferred to nitrocellulose membranes and then immunoreactive proteins were detected as described previously [35]. The dilution factors for majority of antibodies were 1:1000, for V5 it was 1:5000. Immunoreactive proteins were detected using a SuperSignal West Femto Substrate reagent.

2.4. Immunoprecipitation

Immunoprecipitation was performed with rabbit TrueBlot system per manufacturer's instructions or using A/G beads. Approximately 200 μg of total proteins were precleared with 30 μl of A/G for 1 h at 4°C. 3–5 μg of specific antibody was added for 1–3 h incubation at 4°C followed by additional incubation with 30 μl of A/G beads. After incubation beads were spun down and washed 3–5 times with the buffer containing 50 mM HEPES, 150 mM NaCl, 0.5 mM EGTA, 50 mM NaF, 10 mM Na_3VO_4, and 1 mM phenymethylsulfonyl fluoride with 1% [vol/vol] of Triton X-100. The proteins were then released from the beads by boiling in Laemmli buffer for 5 min, separated by SDS-PAGE followed by immunoblot analysis with appropriate antibodies as described previously [35]. Pull down assays were performed by rotation with V5-, His- and GST-CaMKI beads for 2–4 hours at 4°C. The proteins were then also released from the beads by boiling in Laemmli buffer for 5 min and processed for SDS-PAG and immunoblot analysis.

2.5. Construction of CaMKI mutants

Full length and truncated *CaMKI* mutants were constructed as described previously [36]. Briefly, the deletion mutants *CaMKI 181*, *CaMKI 271*, *CaMKI 296* and *CaMKI K59R* and *CaMKI K110R*, harboring point mutations were generated by site-direct mutagenesis using similar PCR-based strategies with appropriate forward and reverse primers, using His- and V_5-double tagged CaMKI plasmid as a template.

2.6. Expression of recombinant proteins and siRNA

All plasmids were delivered into the cells by nucleofection using electroporation instrument AMAXA or transfection using FuGENE6 protocol. Transfections with FuGENE6 were performed in serum-free medium for 24 h. For siRNA or shRNA studies cells were transfected with 100 ng of targeted and control RNA using Lipofectamin 2000. Cells were then harvested after 48 h of incubation.

2.7. Immunofluorescence microscopy

MLE cells were cultured on 35 mm MetTek glass-bottom dishes. Cells were then fixed with 4% of paraformaldehyde for 20 min and processed for immunocytochemical staining. For detection of endogenous proteins dilutions used for primary antibodies were 1:250 – 1:500. Alexa 488 or Alexa 647 was used as secondary antibodies at 1:1000 dilutions. The nuclear marker, DAPI was used for visualizing the nuclei. In some studies cells were transfected with GFP-tagged proteins. Cell imaging was performed on a Nikon A1 confocal microscope.

2.8. In vitro TnT and pull-down assays

For *in vitro* synthesis, His-tagged *CaMKI* constructs were added to the rabbit reticulocyte lysate and incubated with T7 RNA polymerase in a 50 μl reaction following the

manufacturer's instructions. *In vitro* synthesized proteins were then processed for pull down with His-conjugated Talon resin. The His-beads conjugated to CaMKI constructs were then washed and used for binding assays.

2.9. Cell cycle analysis

Cells transfected with *Fbxl12* and *LacZ* plasmids were incubated with BrdU (5-bromo-2′-deoxyuridine; 20 mM) for 40 min. MLE cells were then fixed and stained following the manufacturer's instructions (BD Biosciences). Fluorescence-activated cells sorter (FACS) samples were analyzed with the Accuri C6 system. DNA content was analyzed using FCS3 express software (De NOVO Software).

2.10. In vitro ubiquitin conjugation assays

The ubiquitination of V5-CaMKI was performed in a volume of 25 μl containing 50 mM Tris pH 7.6, 5 mM $MgCl_2$, 0.6 mM DTT, 2 mM ATP, 1.5 ng/μl E1, 10 ng/μl Ubc5, 10 ng/μl ubiquitin, 1 μM ubiquitin aldehyde, 4–16 μl of purified Cullin1, Skp 1, Rbx 1 and Fbxl12. Reaction products were processed for V5 immunoblotting.

2.11. Statistical analysis

Statistical analysis was performed by one-way analysis of variance or Student's test. Data are presented as mean±SE.

3. Results

3.1. Fbxl12 triggers CaMKI degradation thereby disrupting cyclin D1/cdk4 complex assembly

The molecular control of CaMKI protein stability remains largely unknown. To assess this, we first expressed SCF-based plasmids encoding F box proteins of the FBXL family (Fig. 1A) and FBXO and FBXW families (data not shown) in a murine lung epithelial (MLE) cell line. Effectiveness of V5 tagged F-box protein expression was analyzed by immunoblotting (Fig. 1A, upper blot). CaMKI protein was most efficiently degraded by Fbxl12, a protein upregulated during TGF-β-induced G1 arrest [4]. *Fbxl12* plasmid effects were selective, as its expression did not alter immunoreactive PKCα or p38α/β levels (Fig. 1A). Transfection with increasing amounts of *Fbxl12* plasmid was sufficient to mediate degradation of CaMKI in a dose-dependent manner unlike CaMKII (Fig. 1B). To evaluate if CaMKI degradation might cause G1 arrest we overexpressed *Fbxl12* and *LacZ* plasmids in cells labeled with BrdU and performed analysis by 2-color flow cytometry (Fig. 1C). Expression of *Fbxl12* plasmid, unlike control plasmid, increased the relative proportion of cells within the G1 phase (Fig. 1C). These effects were not associated with increased cellular apoptosis (data not shown). We next examined cyclin D1/ cdk4 complex formation in the cells after *Fbxl12* plasmid expression. Here, immunoprecipitation using cdk4 antibodies followed by cyclin D1 immunoblotting revealed a significant loss of cyclin D1 in the complex after *Fbxl12* plasmid expression (Fig. 1D). This effect was recapitulated using CaMKI shRNA where CaMKI depletion in cells significantly decreased levels of immunoreactive cdk4 in the complex compared to cells expressing control shRNA (Fig. 1E). These results suggest that elimination of CaMKI by Fbxl12 mediated degradation or CaMKI knockdown induces G1 arrest via impaired assembly of the cyclin D1/cdk4 complex in lung epithelia. In addition, several treatments that are known as G1 arrest inducers [37,38,39,40] up-regulated FBXL12 which was correlated with significant loss of CaMKI expression (Fig. 1F).

3.2. Fbxl12 binds CaMKI directly to trigger its degradation

We next examined CaMKI half-life after Fbxl12 overexpression (Fig. 2A) and knockdown (Fig. 2B). Overexpression of *Fbxl12* plasmid compared to control plasmid significantly decreased CaMKI half-life (Fig. 2A), whereas knockdown of Fbxl12 using siRNA increased CaMKI lifespan (Fig. 2B). MG132, a proteasomal inhibitor, stabilized CaMKI levels unlike leupeptin, a lysosomal inhibitor (Fig. 2C). Endogenous Fbxl12 and CaMKI interacted as demonstrated after Fbxl12 immunoprecipitation followed by immunoblot analysis with CaMKI antibodies using lysates of cells exposed to Ca^{2+} or lipopolysaccharide (LPS), or cells transfected with *CaMKI* plasmid (Fig 2D). Indeed, Ca^{2+} decreased binding between CaMKI and Fbxl12 whereas LPS, that blocks cell proliferation causing G1 arrest [41,42], induced CaMKI-Fbxl12 association (Fig. 2D). Further, ectopic expression of control plasmid, *LacZ*, or *V5-Fbxl12* plasmid followed by pull down assays using V5-beads showed that CaMKI and Fbxl12 were bound consistent with results obtained by co-immunoprecipitation (Fig. 2E). Thus, both endogenous and ectopically expressed FBXL2 interact with CaMKI. Last, Fbxl12 and CaMKI co-localized in the cytoplasm of MLE cells under unstimulated conditions and after Ca^{2+} or LPS exposure (Fig. 2F).

3.3. Fbxl12 targets CaMKI for ubiquitination

To demonstrate that CaMKI is ubiquitinated we performed immunoprecipitation using CaMKI antibodies (Fig. 3A) followed by immunoblotting with anti-ubiquitin antibodies (Fig. 3A). To support these observation we also used immunoprecipitation with V5 antibodies in the cells co-expressed V5-CaMKI and HA-ubiquitin (Fig. 3B). *In vitro* ubiquitination assays with inclusion of purified recombinant SCF^{Fbxl12} with addition of ubiquitin, E1, and E2 enzymes revealed that the reactions generated polyubiquitinated CaMKI (Fig. 3C). To identify the ubiquitination acceptor site(s) within CaMKI, we constructed V5-tagged carboxyl-terminal deletion mutants, expressed the plasmids in MLE cells before exposure to MG132 and analysis by V5 immunoblotting (Fig. 3D, E). F-box proteins are the receptors that usually recruit phosphorylated substrates targeting their phosphodegrons. CaMKI is activated via binding to CaM and following phosphorylation at Thr177. In addition, the CaMKI294/296 truncated mutants unlike the other downstream mutants lacking CaM-binding site are the only mutants that can stay active and phosphorylated at Thr177 without binding to CaM [43]. Thus, we designed the C-terminal truncation mutants that allowed the Fbxl12 binds CaMKI to identify potential ubiquitination site within this kinase. The appearance of polyubiquitinated CaMKI full-length (FL) and other polyubiquitinated constructs (CaMKI181, CaMKI271, CaMKI296) suggested that the ubiquitination acceptor site may be localized within a NH_2-terminal region of the kinase upstream of its phosphodegron that encompass residues Pro171 to Thr181 (Fig. 3E). Expression of point mutations at candidate lysines within the NH_2-terminal region of CaMKI in cells suggested that Lys59 might be a putative ubiquitination site for CaMKI (Fig. 3F, G). This CaMKI variant exhibited a significantly extended half-life compared to CaMKI FL (Fig. 3H, I). The co-expression of *Fbxl12* plasmid with either *CaMKI FL* or *CaMKI K59R* plasmids led to degradation of CaMKI FL, but not the CaMKI K59R mutant (Fig. 3J). Thus, CaMKI appears to be polyubiquitinated at K59 and degraded via the proteosomal pathway in lung epithelium.

3.4. CaMKI controls cell cycle progression in lung epithelia via regulation of phosphorylation and subcellular localization of p27

Mitogen-activated Ca^{2+} influx from the extracellular medium is a key stimulus that regulates cell proliferation via rapid activation CaM-dependent kinases [9,44,45,46,47]. To evaluate the role of CaMKI in G1 progression and assembly of the cyclin D1/cdk4 complex by p27, we first transfected A549 cells (Fig. 4B) or MLE cells (data not shown) with *LacZ*, *CaMKI*

or *Fbxl12* plasmids. Cells were then synchronized to G0 by serum depletion for 48 h and released by addition of 10% serum. The percent of S phase at all time-points analyzed by flow cytometry is indicated at the top of panels Fig. 4A–C. The levels of signaling proteins were then analyzed by immunoblotting. Overexpression of *CaMKI* plasmid prolonged cell cycle progression evidenced by acceleration of the transition from G0 to the S phase, accumulation of S-phase population and robust time-dependent expression of cdk4, cyclin D1 and p27 levels in MLE and A549 cells during 24 h of analysis (Fig. 4B). By comparison, *Fbxl12* plasmid expression induced degradation of CaMKI, reduced cyclin D1 levels, and increased late phase p27 accumulation (Fig. 4C) compared to control (*LacZ*)(Fig. 4A). Phosphorylation of p27 at S10 that is necessary for its nuclear export at G0/G1 followed by its phosphorylation at Thr157 and Thr198 in human cells regulates assembly of cyclin D1/cdk4 at early G1 [28,29]. p27 phosphorylation levels in control cells (*LacZ*) and cells overexpressing *CaMKI* plasmid were correlated with CaMKI activation during cell cycle progression (Fig. 4A–B). After exposing cells to FBS the maximum phosphorylation of p27 at Thr157 and Thr198 in control cells was detected at 6–12 h (Fig. 4A) whereas *CaMKI* overexpression stabilized its phosphorylation from 2 to 12 h (Fig. 4B). Overexpression of *Fbxl12* plasmid totally abrogated p27 phosphorylation at Thr157 and Thr198 in further support that CaMKI might be involved in p27 phosphorylation (Fig. 4C). The levels of Fbxl12 increased in a time-dependent manner in control cells which generally correlated with down-regulation of CaMKI (Fig. 4A). Interestingly, overexpression of *CaMKI* plasmid significantly decreased Fbxl12 levels (Fig. 4B) reflecting an inverse relationship between these proteins during cell cycle progression. Formation of the cdk4/cyclinD1/p27 complex increases during early G1 [29]. Consistent with this our results show increasing expression of these proteins during this time frame in control and CaMKI overexpressing cells (Fig. 4A–B). Moreover, Fbxl12 overexpression induced G1 arrest in these cells and could impair cdk4/cyclinD1/p27 complex assembly via abrogation of Thr157 and Thr198 phosphorylation (Fig. 4C).

To assess subcellular localization of endogenous p27 in lung epithelia *LacZ, CaMKI and Fbxl12* plasmids were expressed in cells as was described above. Localization of endogenous p27 and p-CaMKI were analyzed over time (0–24h) (Fig. 4D–G). Localization of phosphorylated CaMKI (p-CaMKI) in the control cells and cells overexpressing CaMKI did not change at indicated times, whereas the expression of CaMKI was very weak in the cells overexpressing Fbxl12 (Fig. 4D–G). Localization of p27 in control cells was nuclear at G0 and then translocated to cytoplasm, whereas p27 in the cells with overexpressing CaMKI was distributed between the cytoplasm and the nucleus at Go and then at later time points was mostly cytoplasmic. However, in the Fbxl12-expressing cells p27 was predominantly mislocalized in the nucleus at most time points. Thus, these data suggest that CaMKI might also regulate p27 subcellular localization in lung epithelia. These observations were confirmed by additional experiments after transfection of Myc-, Flag- or GFP-tagged p27 in cells (Fig. 6–8).

3.5. CaMKI regulates assembly of cyclin D1/cdk4 via association with p27

We first performed the pull down of p27 from A549 cells overexpressing *LacZ, CaMKI* or *Fbxl12* plasmid using CaMKI-conjugated beads. The binding was monitored by immunodlotting (Fig. 5A–C). Here, we observed time-dependent association of CaMKI with phosphorylated forms of p27. The results demonstrate that overexpression of CaMKI accelerates and extends the time of CaMKI-p27 association that also correlates with p27 phosphorylation levels (Fig. 5B). However, Fbxl12 overexpression significantly abrogates the level of p27 associated with CaMKI and phosphorylation (Fig. 5C). Immunoprecipitation assays also supported these observations (data not shown). The association of p27 and CaMKI was also confirmed by pull down assays using the purified

recombinant protein p27 and CaMKI-conjugated beads (Fig. 5D). These studies show that KN-93, a CaMKI inhibitor significantly abrogated p27-CaMKI interaction (Fig. 5D). Other pull down assays performed with CaMKI-conjugated beads using lysates from MLE cells exposed to KN-93 or Ca^{2+} also demonstrated that the inhibitor significantly abrogated binding of CaMKI to p27 (Fig. 5E). The pull down of CaMKI from *LacZ*-, *CaMK*- or *Fbxl12*-transfected cells using p27-conjugated beads also revealed that the expression of Fbxl12 reduced the level of CaMKI associated with the beads (Fig. 5F). Immunoprecipitation from these cells using cdk4 antibody (Fig. 5G–I) followed by immunoblot analysis with p27 and cyclin D1 antibodies demonstrated that *CaMKI* compared to *LacZ* plasmid expression induced cdk4/cyclin D1/p27 complex formation at all indicated times compared to control (Fig. 5G, H). Overexpression of *Fbxl12* plasmid greatly reduced cyclin D1 detected within the complex (Fig. 5I). The binding was monitored at the time when p27 was maximally co-localized with CaMKI as was previously shown (Fig. 4).

3.6. CaMKI phosphorylates p27 regulating its subcellular localization in human lung epithelia

To test our hypothesis that CaMKI phosphorylates p27 at Thr157 and Thr198 we first made a sequence alignment of the CaMKI recognition consensus site with sequences within p27 that included Thr157 and Thr198. Sequence alignment demonstrates that the motif is noncanonical but partially resembles a CaMKI consensus sequence (Fig. 6A, Fig. S1A). We then performed *in vitro* reactions using p27 an active or inactive forms of CaMKI with Ca^{2+}. Immunoblot analysis using phospho-specific p27 Thr157 and p27 Thr198 antibody revealed that only an active form of CaMKI was able to robustly phosphorylate p27 *in vitro* (Fig. 6B). To support this observation A549 cells were transfected with plasmids encoding *Myc-tagged p27 wild-type* (WT) or two point mutants, *Myc-p27T157A* and *Myc-p27T198A* followed by pull down with anti-Myc agarose. The Myc-conjugated p27 WT and p27 mutants were then dephosphorylated with alkaline phosphatase followed by phosphorylation with CaMKI in presence of [γ ^{32}-P]-ATP, Ca^{2+} and CaM (Fig. 6C). The results reveal that mutations of both sites reduced p27 phosphorylation with the p27T198A mutation exhibiting significantly lower levels of phosphorylation (Fig. 6C). To test if the phosphorylation at T157 and T198 would affect cdk4/cyclinD1/p27 complex formation, A549 cells were co-transfected with V5-*CaMKI* and either *Myc-p27WT*, *Myc-p27T157A*, or *Myc-p27T198A* plasmids followed by V5 immunoprecipitation (Fig. 6D). Here, expression of both p27 mutants reduced complex formation evidenced by loss of cdk4 and cyclin D1 (Fig. 6D). A549 cells co-transfected as described above were also starved and then released with FBS followed by immunostaining (Fig. 6E–G). The results show that serum addition and overexpression of CaMKI had no effect on the subcellular localization of mutants. Both p27 T157A and p27 T198A mutants were predominantly nuclear at indicated time points, whereas the p27 WT protein translocated to the cytoplasm in response to serum addition or CaMKI overexpression (Fig. 6E–G). Localization of endogenous p27 phosphorylated at T157 (Fig. S2A–D) and T198 (Fig. S3A–D) in A549 cells transfected with *LacZ*, *CaMKI* or *Fbxl12* plasmids in response to serum was also visualized by immunostaining. The results confirm our findings revealing CaMKI-dependent localization of mutants in the cells. Thus, CaMKI triggers p27 phosphorylation at T157 and T198 sites that stabilize the cdk4/cyclinD1/p27 complex and regulate p27 intracellular localization in human lung epithelia.

3.7. CaMKI phosphorylates p27 regulating its subcellular localization in mouse lung epithelia

By sequence alignment, T157 is absent in mouse p27, whereas T198 in human sequence is corresponding to T197 in mouse p27 (Fig. S1A–C). To verify if CaMKI can phosphorylate p27 purified from mouse cells we performed *in vitro* phosphorylation reactions as above (Fig. 7A). Only an active form of CaMKI was able to phosphorylate p27. Thus, CaMKI

phosphorylates human and mouse p27. Analysis of the mouse p27 sequence reveals two non-canonical motifs with partial resemblance to a CaMKI consensus recognition signature (Fig. 7B). T170 and T197 are phosphorylated by AMPK [48,49]. These phosphorylation sites regulate p27 cellular localization [48,49]. To investigate if CaMKI can phosphorylate mouse p27 at these two sites, MLE cells were transfected with *p27 WT*, *p27 T170A*, *p27 T197A*, or *p27 T170A/T197A*-Flag-tagged mutant plasmids followed by pull down with Flag-agarose. Agarose beads conjugated to *Flag-p27WT*, *Flag- p27T170A*, *Flag-p27T197A* and *Flag-p27T170A/T197A* were then dephosphorylated with alkaline phosphatase and used in phosphorylation reactions with CaMKI in the presence of [γ ^{32}-P]-ATP, Ca^{2+} and CaM. The results show that mutations of both sites significantly reduced p27 phosphorylation, whereas the double mutant exhibited total loss of ability to be phosphorylated by CaMKI (Fig. 7C). Co-expression of *His-CaMKI* plasmid with either Flag-tagged *p27 WT* or various p27 mutant plasmids followed by pull down assays using His-conjugated beads revealed significantly decreased binding of p27 mutants with CaMKI in contrast to p27 WT (Fig. 7D).

To investigate if phosphorylation of p27 at T170 and T197 sites by CaMKI can regulate its intracellular localization, MLE cells were co-transfected with *CaMKI* plasmid and either Flag-tagged *p27 WT* or p27 mutant plasmids as described above. Cells were then starved and finally released with serum addition followed by immunostaining at indicated times (Fig. 7E–G). The results demonstrate that both p27T170A and p27T197A mutants were nuclear whereas p27 WT translocated to the cytoplasm in response to serum and CaMKI overexpression (Fig. 7E–G). Thus, CaMKI might regulate p27 intracellular localization in mouse lung epithelia via phosphorylation of this protein at T170 and T197 sites.

3.8. Crosstalk between CaMKI and AKT on p27 phosphorylation

CaMKI and AKT are phosphorylated by upstream activators, and CaMKK becomes active after elevation of Ca^{2+} within minutes [50]. Serum addition to quiescent cells immediately (3–20 sec.) induces influx of extracellular Ca^{2+} [50]. CaMKI, a primary substrate of CaMKK, can be activated in less than 5 min, whereas PKB/AKT, is a secondary substrate because its activation by CaMKK is slow (~ 1 h) [51]. To evaluate the possible relationship between CaMKI and AKT on p27 phosphorylation during the cell cycle, we first analyzed time-dependent activation of CaMKI, AKT, and p27 during cell cycle progression. Immunoblot analysis demonstrated maximal expression of CaMKI within the first 30 min after serum addition whereas AKT was stably expressed at all indicated time points in MLE cells (Fig. 8A). The activated form of CaMKI was detected in 5 min after serum addition and remained active at all indicated time points with variations between 5 min to 6 h. However, AKT activation at both sites (S473 and T308) that are necessary to confer its fully activated form was time dependent. Phosphorylation of p27 at T157 increased from 15 min to 6 h whereas phosphorylation at T198 was detected later after release from G0 (Fig. 8A). Total levels of p27 were maximal from 1 to 6 h. Formation of p27-cyclin D1/cdk4 complexes and p27 phosphorylation at T157 and T198 increased during early G1 from 2 to 6 h as shown above (Fig. 4, 6) and temporally was linked to activation of CaMKI and AKT (Fig. 8A). Thus, both kinases can phosphorylate p27 at these sites (T157 and T198) and induce cyclin D1/cdk4 complex formation. However the active form of CaMKI appeared prior to AKT activation. Thus, to evaluate which kinase is upstream to phosphorylate p27 we exposed MLE cells to the CaMKK inhibitor, STO-609, the CaMKI inhibitor, KN-93 or LY294002, a known AKT inhibitor (Fig. 8B–E). The results show that both kinases are sensitive to these inhibitors. These observations suggest that CaMKI and AKT actions might be modulated by Ca^{2+}. To test this hypothesis we exposed cells to the Ca^{2+} chelator, EGTA, and then immunoprecipitated CaMKI and AKT using p27 antibodies. Immunoblot analysis demonstrated that binding of CaMKI and AKT to p27 and its phosphorylation by these

kinases dramatically depends on Ca^{2+} (data not shown). Overexpression of CaMKI or AKT in A549 cells shows that FBS-induced p27 phosphorylation correlates with CaMKI and AKT activation (Fig. S4A, B). However, phosphorylation of p27 by AKT exhibited a slight delay compared to phosphorylation by CaMKI (Fig. S4A, B). In addition, overexpression of Fbxl12 in the cells regulated AKT intracellular localization by induction of its nuclear translocation (Fig. S4C). Finally, *GFP-p27* plasmid was transfected or co-transfected with *CaMKI* plasmid into MLE cells followed by starvation for 48 h. Cells were then pulsed with 10% FBS or Ca^{2+} and fixed at indicated times followed by immunostaining (Fig. 8F, G). The results show that both treatments induced time-dependent p27 cytoplasmic translocation in a similar manner. Immunoblot analysis demonstrated comparable activation of CaMKI and AKT by these agents with a little delay in activation of AKT (Fig. 8H, I). Thus, these data are compatible with the idea that CaMKI pathway is upstream of AKT and that CaMKI might be a prime activator of p27.

4. Discussion

The CaMK family of serine/threonine kinases plays an essential role in cell cycle progression [11]. The molecular regulation of CaMKI, a key member of this family that controls G1 progression through regulation of cyclin D1/cdk4 complexes [18], is poorly characterized at the level of protein stability. These studies are the first demonstration of CaMKI degradation by the proteosomal pathway mediated by the F box protein, Fbxl12. CaMKI was shown to be a direct substrate for Fbxl12 and modulation of this SCF component altered cell cycle progression and cyclin D1/cdk4 complex assembly through CaMKI abundance. Moreover, our studies support a mechanism by which Fbxl12 via CaMKI degradation mediates G1 arrest. Here, CaMKI regulates cyclin D1/cdk4 complex formation by triggering phosphorylation of p27, which mediates assembly, activation and cytoplasmic localization of cyclin D-cdk. [17,52,53]. As a whole, these observations suggest that critical a SCF component (Fbxl12) acting through CaMKI may control cell fate and replicative capacity.

Here, we provide evidence that p27 is a potential substrate for CaMKI. Phosphorylation of p27 at Thr157 and Thr198 sites stabilizes the cyclin D1/cdk4 complex and regulates its activation during G1 [28,29,54]. In quiescent cells p27 is localized in the nucleus but following mitogen-stimulated nuclear export in early G1, p27 is needed to promote cyclin D1/cdk4 assembly. For its cytoplasmic retention p27 is phosphorylated at serine 10 that facilitates binding to exportin 1 required for p27 cytoplasmic translocation and G1 progression [27,55]. Phosphorylation at serine 10 is coordinated through concerted actions of a number of kinases and cytoplasmic retention is affected by the molecular chaperone 14-3-3 [23,28,56]. For example, p27 phosphorylation at T157and T198 in the cytoplasm is mediated by AKT that also influences G1 progression [57,58,59]. However, a number of studies demonstrate that mitogen-induced Ca^{2+} elevations in cells trigger rapid activation of the CaMK cascade [44,60,61,62]. CaMKI is required for G1 progression via regulation of cyclin D1/cdk4 complexes, but how this kinase controls assembly of these proteins is unknown. Our results demonstrate that CaMKI was rapidly activated by serum and its activation correlated with p27 phosphorylation at Thr157 and Thr198 in human lung epithelia (Fig. 4A, Fig. 8A). Overexpression of CaMKI accelerated and prolonged p27 phosphorylation, whereas degradation of CaMKI mediated by Fbxl12 dramatically reduced p27 phosphorylation at these molecular sites (Fig. 4B,C). These observations were also confirmed by investigation of p27 intracellular localization during cell cycle progression (Fig. 4D–G). We demonstrate that overexpression of CaMKI accelerated the formation of cyclin D1/cdk4 complexes, whereas this assembly was reduced via Fbxl12-induced CaMKI degradation (Fig. 1D, E; 5G, I). *In vitro* phosphorylation assays showed that CaMKI phosphorylates p27 at Thr157 and Thr198 in human cells (Fig. 6B, C); an effect reduced

using p27 Thr157 and Thr198 point mutants. Further, phosphorylation of human p27 at these sites regulated its intracellular localization (Fig. 6E–G, Fig. S2–3). Collectively, these results suggest that CaMKI is involved in mediating G1 progression by promoting cyclin D1/cdk4 complex formation through site-specific p27 phosphorylation in human lung epithelia.

The p27 NLS that includes a stretch between 151–163 residues can regulate p27 intracellular localization via phosphorylation of residues within or juxtaposed near an NLS [63]. For example, AMP-activated protein kinase (AMPK) can phosphorylate p27 at T170 located close to the p27 NLS and control its cellular localization [48]. AMPK-mediated phosphorylation of p27 at T197 induces binding to 14-3-3 and increases its stability in a murine Tsc2-null tumor cell line [49]. Indeed, T170 and T197 are attractive sites for CaMKI that have some similarities to a consensus phosphorylation sequence recognized by CaMKI (Fig. 7B). Our studies demonstrate that CaMKI phosphorylates Thr170 and Thr197 within murine p27 to regulate its subcellular localization in mouse lung epithelia (Fig. 7). Thus, the data suggest that CaMKI might be a regulator of G1 progression in mouse lung epithelia via phosphorylation of p27. We also believe that CaMKI can phosphorylate Thr170 within human p27.

Since, AKT regulates G1 progression in cells its raises the possibility of crosstalk between AKT and CaMKI induced p27 phosphorylation. The immediate Ca^{2+} influx that occurs in response to mitogen stimulation plays a significant role in cell cycle and its blockade in the early G1 phase leads to reduction in cellular proliferation [44]. External Ca^{2+} influx through the Ca^{2+} channels is important and sufficient for cell cycle progression that leads to activation of critical signaling events upstream of CaMKs [60,61,64]. The Ca^{2+} channel blocker, amlodipine stimulates G1 arrest and growth inhibition via reduction of cyclin D1 and cdk4 protein levels, inhibition of cdk/cyclin-associated kinase activities, reduction of pRb and induction of p21(Waf1/Cip) expression [65]. Expression of Ca^{2+} channels depends on the stage of the cell cycle but it is usually higher during G1 [45]. Thus, Ca^{2+} is an essential mitogenic stimulus. Our studies show that Ca^{2+} is involved in p27 intracellular localization and is sufficient to activate CaMKI and AKT comparable to serum stimulation (Fig. 8F–I). The Ca^{2+} signaling system triggers the cell cycle through activation of the Ca^{2+}/CaM-dependent protein kinase cascade to catalyze critical phosphorylation events [66,67,68,69]. Binding of Ca^{2+}/CaM to CaMKI exposes its activation loop site to allow phosphorylation by the upstream CaMKK that becomes active within a minutes after mitogen exposure; concomitantly, Ca^{2+}/CaM engagement to CaMKI also activates secondary targets such as AKT [51] and AMPK [70,71,72,73]. This was reflected in our experiments where AKT activation exhibited a slight delay in comparison to CaMKI activation (Fig. 8A, H, I; Fig. S4A, B). CaMKI and AKT are multifunctional kinases involved in many cellular signaling pathways that are seldom linear and often form complex networks with other signaling pathways. This crosstalk can occur at several levels; indeed there can be direct phosphorylation between protein kinases or regulatory phosphorylation of either an upstream or downstream effectors. Thus, crosstalk between the CaMKI and PKB/AKT signaling pathways may reflect a very important communication network. In spite of p27 phosphorylation at T157 and T198 as candidate sites for both kinases the activation of CaMKI occurs earlier than AKT (Fig. 8A, H). It was recently demonstrated that serum addition immediately causes transient nuclear localization of AKT [28]. Because phosphorylation of p27 at Thr157 is a cytoplasmic event, the authors speculate that p27 requires another cytosolic factor that acts in concert with AKT [28]. CaMKI is a predominantly cytosolic protein. Thus, based on our results, CaMKI might be an upstream kinase that primes p27 for subsequent phosphorylation by AKT. It is also possible that these two kinases can be regulated via different upstream pathways by different hormones or growth factors included in serum. In addition, the CaMKI cascade might also participate in

cross talk with other signaling pathways; CaMKK/CaMKI might activate the AMP-activated protein kinase pathway, the mitogen-activated protein kinase pathway, or the c-AMP-dependent protein kinase [74]. However, more research is required to determine how these pathways act and are coordinately regulated.

In conclusion, our report is the first discover that an ubiquitin E3 ligase component, F-box protein Fbxl12, mediates CaMKI degradation via a proteasome-directed pathway. These studies also reveal a new CaMKI substrate, $p27^{Kip1}$. We have demonstrated that CaMKI phosphorylates p27 at specific sites Thr157 and Thr198 in human cells and at Thr170 and Thr197 in mouse cells which is critical for cdk4/cyclin D1 complex formation and p27 intracellular localization. This is the first description uncovering a mechanistic pathway whereby CaMKI participates in cdk4/cyclin D1 complex during G1 progression. Lastly, the activation of CaMKI during G1 transition followed by p27 phosphorylation appears to be upstream to p27 phosphorylation by other kinases. Thus, our report unveils the following novel discoveries regarding a relatively new F-box protein, Fbxl12, an E3 ligase component and how it controls availability of the new substrate, CaMKI, which impacts cell cycle progression. We also believe that these studies provide a significant conceptual and mechanistic advance in the understanding of the molecular physiology related to cell cycle processes and might be used for mechanism-based therapy.

Supplementary Material

Refer to Web version on PubMed Central for supplementary material.

Acknowledgments

We greatly appreciate Cheryl Lyn Walker, Director of Institute of Biosciences & Technology Center for Translational Cancer Research of University of Texas's kind gift *p27WT*, *p27T170A*, *p27T197A* and *p27T170A/197A* plasmids. This material is based upon work supported, in part, by the US Department of Veterans Affairs, Veterans Health Administration, Office of Research and Development, Biomedical Laboratory Research and Development. This work was supported by a Merit Review Award from the US Department of Veterans Affairs and National Institutes of Health R01 grants HL096376, HL097376 and HL098174 (to R.K.M.), HL116472 (to B.B.C.) and American Heart Association (AHA) awards 12SDG9050005 (J.Z.). The contents presented do not represent the views of the Department of Veterans Affairs or the United States Government.

References

1. Massague J. G1 cell-cycle control and cancer. Nature. 2004; 432:298–306. [PubMed: 15549091]
2. Kipreos ET, Pagano M. The F-box protein family. Genome Biol. 2000; 1:REVIEWS3002. [PubMed: 11178263]
3. Santra MK, Wajapeyee N, Green MR. F-box protein FBXO31 mediates cyclin D1 degradation to induce G1 arrest after DNA damage. Nature. 2009; 459:722–725. [PubMed: 19412162]
4. Kim M, Nakamoto T, Nishimori S, Tanaka K, Chiba T. A new ubiquitin ligase involved in p57KIP2 proteolysis regulates osteoblast cell differentiation. EMBO Rep. 2008; 9:878–884. [PubMed: 18660753]
5. Chen BB, Glasser JR, Coon TA, Zou C, Miller HL, et al. F-box protein FBXL2 targets cyclin D2 for ubiquitination and degradation to inhibit leukemic cell proliferation. Blood. 2012; 119:3132–3141. [PubMed: 22323446]
6. Chen BB, Glasser JR, Coon TA, Mallampalli RK. F-box protein FBXL2 exerts human lung tumor suppressor-like activity by ubiquitin-mediated degradation of cyclin D3 resulting in cell cycle arrest. Oncogene. 2012; 31:2566–2579. [PubMed: 22020328]
7. Hickie RA, Wei JW, Blyth LM, Wong DY, Klaassen DJ. Cations and calmodulin in normal and neoplastic cell growth regulation. Can J Biochem Cell Biol. 1983; 61:934–941. [PubMed: 6354400]
8. Kahl CR, Means AR. Regulation of cell cycle progression by calcium/calmodulin-dependent pathways. Endocr Rev. 2003; 24:719–736. [PubMed: 14671000]

9. Short AD, Bian J, Ghosh TK, Waldron RT, Rybak SL, et al. Intracellular Ca2+ pool content is linked to control of cell growth. Proc Natl Acad Sci U S A. 1993; 90:4986–4990. [PubMed: 8389460]
10. Joseph JD, Means AR. Identification and characterization of two Ca2+/CaM-dependent protein kinases required for normal nuclear division in Aspergillus nidulans. J Biol Chem. 2000; 275:38230–38238. [PubMed: 10988293]
11. Skelding KA, Rostas JA, Verrills NM. Controlling the cell cycle: the role of calcium/calmodulin-stimulated protein kinases I and II. Cell Cycle. 2011; 10:631–639. [PubMed: 21301225]
12. Goldberg J, Nairn AC, Kuriyan J. Structural basis for the autoinhibition of calcium/calmodulin-dependent protein kinase I. Cell. 1996; 84:875–887. [PubMed: 8601311]
13. Matsushita M, Nairn AC. Characterization of the mechanism of regulation of Ca2+/ calmodulin-dependent protein kinase I by calmodulin and by Ca2+/calmodulin-dependent protein kinase kinase. J Biol Chem. 1998; 273:21473–21481. [PubMed: 9705275]
14. Morris TA, DeLorenzo RJ, Tombes RM. CaMK-II inhibition reduces cyclin D1 levels and enhances the association of p27kip1 with Cdk2 to cause G1 arrest in NIH 3T3 cells. Exp Cell Res. 1998; 240:218–227. [PubMed: 9596994]
15. Rodriguez-Mora OG, LaHair MM, McCubrey JA, Franklin RA. Calcium/calmodulin-dependent kinase I and calcium/calmodulin-dependent kinase kinase participate in the control of cell cycle progression in MCF-7 human breast cancer cells. Cancer Res. 2005; 65:5408–5416. [PubMed: 15958590]
16. Takai N, Ueda T, Nasu K, Yamashita S, Toyofuku M, et al. Targeting calcium/calmodulin-dependence kinase I and II as a potential anti-proliferation remedy for endometrial carcinomas. Cancer Lett. 2009; 277:235–243. [PubMed: 19168280]
17. Ciarallo S, Subramaniam V, Hung W, Lee JH, Kotchetkov R, et al. Altered p27(Kip1) phosphorylation, localization, and function in human epithelial cells resistant to transforming growth factor beta-mediated G(1) arrest. Mol Cell Biol. 2002; 22:2993–3002. [PubMed: 11940657]
18. Kahl CR, Means AR. Regulation of cyclin D1/Cdk4 complexes by calcium/calmodulin-dependent protein kinase I. J Biol Chem. 2004; 279:15411–15419. [PubMed: 14754892]
19. Liang J, Zubovitz J, Petrocelli T, Kotchetkov R, Connor MK, et al. PKB/Akt phosphorylates p27, impairs nuclear import of p27 and opposes p27-mediated G1 arrest. Nat Med. 2002; 8:1153–1160. [PubMed: 12244302]
20. Florenes VA, Lu C, Bhattacharya N, Rak J, Sheehan C, et al. Interleukin-6 dependent induction of the cyclin dependent kinase inhibitor p21WAF1/CIP1 is lost during progression of human malignant melanoma. Oncogene. 1999; 18:1023–1032. [PubMed: 10023678]
21. Slingerland J, Pagano M. Regulation of the cdk inhibitor p27 and its deregulation in cancer. J Cell Physiol. 2000; 183:10–17. [PubMed: 10699961]
22. Singh SP, Lipman J, Goldman H, Ellis FH Jr, Aizenman L, et al. Loss or altered subcellular localization of p27 in Barrett's associated adenocarcinoma. Cancer Res. 1998; 58:1730–1735. [PubMed: 9563491]
23. Fujita N, Sato S, Katayama K, Tsuruo T. Akt-dependent phosphorylation of p27Kip1 promotes binding to 14-3-3 and cytoplasmic localization. J Biol Chem. 2002; 277:28706–28713. [PubMed: 12042314]
24. Boehm M, Yoshimoto T, Crook MF, Nallamshetty S, True A, et al. A growth factor-dependent nuclear kinase phosphorylates p27(Kip1) and regulates cell cycle progression. EMBO J. 2002; 21:3390–3401. [PubMed: 12093740]
25. Fujita N, Sato S, Tsuruo T. Phosphorylation of p27Kip1 at threonine 198 by p90 ribosomal protein S6 kinases promotes its binding to 14-3-3 and cytoplasmic localization. J Biol Chem. 2003; 278:49254–49260. [PubMed: 14504289]
26. Kajihara R, Fukushige S, Shioda N, Tanabe K, Fukunaga K, et al. CaMKII phosphorylates serine 10 of p27 and confers apoptosis resistance to HeLa cells. Biochem Biophys Res Commun. 2010; 401:350–355. [PubMed: 20851109]

27. Connor MK, Kotchetkov R, Cariou S, Resch A, Lupetti R, et al. CRM1/Ran-mediated nuclear export of p27(Kip1) involves a nuclear export signal and links p27 export and proteolysis. Mol Biol Cell. 2003; 14:201–213. [PubMed: 12529437]
28. Shin I, Rotty J, Wu FY, Arteaga CL. Phosphorylation of p27Kip1 at Thr-157 interferes with its association with importin alpha during G1 and prevents nuclear re-entry. J Biol Chem. 2005; 280:6055–6063. [PubMed: 15579463]
29. Larrea MD, Liang J, Da Silva T, Hong F, Shao SH, et al. Phosphorylation of p27Kip1 regulates assembly and activation of cyclin D1-Cdk4. Mol Cell Biol. 2008; 28:6462–6472. [PubMed: 18710949]
30. Hara T, Kamura T, Nakayama K, Oshikawa K, Hatakeyama S. Degradation of p27(Kip1) at the G(0)-G(1) transition mediated by a Skp2-independent ubiquitination pathway. J Biol Chem. 2001; 276:48937–48943. [PubMed: 11682478]
31. Malek NP, Sundberg H, McGrew S, Nakayama K, Kyriakides TR, et al. A mouse knock-in model exposes sequential proteolytic pathways that regulate p27Kip1 in G1 and S phase. Nature. 2001; 413:323–327. [PubMed: 11565035]
32. Montagnoli A, Fiore F, Eytan E, Carrano AC, Draetta GF, et al. Ubiquitination of p27 is regulated by Cdk-dependent phosphorylation and trimeric complex formation. Genes Dev. 1999; 13:1181–1189. [PubMed: 10323868]
33. James MK, Ray A, Leznova D, Blain SW. Differential modification of p27Kip1 controls its cyclin D-cdk4 inhibitory activity. Mol Cell Biol. 2008; 28:498–510. [PubMed: 17908796]
34. Wander SA, Zhao D, Slingerland JM. p27: a barometer of signaling deregulation and potential predictor of response to targeted therapies. Clin Cancer Res. 2011; 17:12–18. [PubMed: 20966355]
35. Agassandian M, Chen BB, Schuster CC, Houtman JC, Mallampalli RK. 14-3-3 zeta escorts CCTalpha for calcium-activated nuclear import in lung epithelia. FASEB J. 2010; 24:1271–1283. [PubMed: 20007511]
36. Agassandian M, Chen BB, Pulijala R, Kaercher L, Glasser JR, et al. Calcium-calmodulin kinase I cooperatively regulates nucleocytoplasmic shuttling of CCTalpha by accessing a nuclear export signal. Mol Biol Cell. 2012; 23:2755–2769. [PubMed: 22621903]
37. Hsu SL, Hsu JW, Liu MC, Chen LY, Chang CD. Retinoic acid-mediated G1 arrest is associated with induction of p27(Kip1) and inhibition of cyclin-dependent kinase 3 in human lung squamous carcinoma CH27 cells. Exp Cell Res. 2000; 258:322–331. [PubMed: 10896783]
38. Liu X, Yang JM, Zhang SS, Liu XY, Liu DX. Induction of cell cycle arrest at G1 and S phases and cAMP-dependent differentiation in C6 glioma by low concentration of cycloheximide. BMC Cancer. 2010; 10:684. [PubMed: 21159181]
39. Fiore M, Zanier R, Degrassi F. Reversible G(1) arrest by dimethyl sulfoxide as a new method to synchronize Chinese hamster cells. Mutagenesis. 2002; 17:419–424. [PubMed: 12202630]
40. Mikami K, Haseba T, Ohno Y. Ethanol induces transient arrest of cell division (G2 + M block) followed by G0/G1 block: dose effects of short- and longer-term ethanol exposure on cell cycle and cell functions. Alcohol Alcohol. 1997; 32:145–152. [PubMed: 9105508]
41. Zuniga E, Motran C, Montes CL, Diaz FL, Bocco JL, et al. Trypanosoma cruzi-induced immunosuppression: B cells undergo spontaneous apoptosis and lipopolysaccharide (LPS) arrests their proliferation during acute infection. Clin Exp Immunol. 2000; 119:507–515. [PubMed: 10691924]
42. Xaus J, Cardo M, Valledor AF, Soler C, Lloberas J, et al. Interferon gamma induces the expression of p21waf-1 and arrests macrophage cell cycle, preventing induction of apoptosis. Immunity. 1999; 11:103–113. [PubMed: 10435583]
43. Haribabu B, Hook SS, Selbert MA, Goldstein EG, Tomhave ED, et al. Human calcium-calmodulin dependent protein kinase I: cDNA cloning, domain structure and activation by phosphorylation at threonine-177 by calcium-calmodulin dependent protein kinase I kinase. EMBO J. 1995; 14:3679–3686. [PubMed: 7641687]
44. Barbiero G, Munaron L, Antoniotti S, Baccino FM, Bonelli G, et al. Role of mitogen-induced calcium influx in the control of the cell cycle in Balb-c 3T3 fibroblasts. Cell Calcium. 1995; 18:542–556. [PubMed: 8746952]

45. Kuga T, Kobayashi S, Hirakawa Y, Kanaide H, Takeshita A. Cell cycle--dependent expression of L- and T-type Ca2+ currents in rat aortic smooth muscle cells in primary culture. Circ Res. 1996; 79:14–19. [PubMed: 8925562]
46. Hirakawa Y, Kuga T, Kobayashi S, Kanaide H, Takeshita A. Dual regulation of L-type Ca2+ channels by serotonin 2 receptor stimulation in vascular smooth muscle cells. Am J Physiol. 1995; 268:H544–549. [PubMed: 7864178]
47. Pallotta T, Peres A. Membrane conductance oscillations induced by serum in quiescent human skin fibroblasts. J Physiol. 1989; 416:589–599. [PubMed: 2481733]
48. Short JD, Houston KD, Dere R, Cai SL, Kim J, et al. AMP-activated protein kinase signaling results in cytoplasmic sequestration of p27. Cancer Res. 2008; 68:6496–6506. [PubMed: 18701472]
49. Short JD, Dere R, Houston KD, Cai SL, Kim J, et al. AMPK-mediated phosphorylation of murine p27 at T197 promotes binding of 14-3-3 proteins and increases p27 stability. Mol Carcinog. 2010; 49:429–439. [PubMed: 20146253]
50. Peres A, Zippel R, Sturani E. Serum induces the immediate opening of Ca2+-activated channels in quiescent human fibroblasts. FEBS Lett. 1988; 241:164–168. [PubMed: 2848719]
51. Wayman GA, Lee YS, Tokumitsu H, Silva AJ, Soderling TR. Calmodulin-kinases: modulators of neuronal development and plasticity. Neuron. 2008; 59:914–931. [PubMed: 18817731]
52. Cheng M, Olivier P, Diehl JA, Fero M, Roussel MF, et al. The p21(Cip1) and p27(Kip1) CDK ‘inhibitors’ are essential activators of cyclin D-dependent kinases in murine fibroblasts. EMBO J. 1999; 18:1571–1583. [PubMed: 10075928]
53. Polyak K, Kato JY, Solomon MJ, Sherr CJ, Massague J, et al. p27Kip1, a cyclin-Cdk inhibitor, links transforming growth factor-beta and contact inhibition to cell cycle arrest. Genes Dev. 1994; 8:9–22. [PubMed: 8288131]
54. Wang C, Li N, Liu X, Zheng Y, Cao X. A novel endogenous human CaMKII inhibitory protein suppresses tumor growth by inducing cell cycle arrest via p27 stabilization. J Biol Chem. 2008; 283:11565–11574. [PubMed: 18305109]
55. Ishida N, Hara T, Kamura T, Yoshida M, Nakayama K, et al. Phosphorylation of p27Kip1 on serine 10 is required for its binding to CRM1 and nuclear export. J Biol Chem. 2002; 277:14355–14358. [PubMed: 11889117]
56. De Vita F, Riccardi M, Malanga D, Scrima M, De Marco C, et al. PKC-dependent phosphorylation of p27 at T198 contributes to p27 stabilization and cell cycle arrest. Cell Cycle. 2012; 11:1583–1592. [PubMed: 22441823]
57. Larrea MD, Wander SA, Slingerland JM. p27 as Jekyll and Hyde: regulation of cell cycle and cell motility. Cell Cycle. 2009; 8:3455–3461. [PubMed: 19829074]
58. Larrea MD, Hong F, Wander SA, da Silva TG, Helfman D, et al. RSK1 drives p27Kip1 phosphorylation at T198 to promote RhoA inhibition and increase cell motility. Proc Natl Acad Sci U S A. 2009; 106:9268–9273. [PubMed: 19470470]
59. Besson A, Gurian-West M, Chen X, Kelly-Spratt KS, Kemp CJ, et al. A pathway in quiescent cells that controls p27Kip1 stability, subcellular localization, and tumor suppression. Genes Dev. 2006; 20:47–64. [PubMed: 16391232]
60. Ufret-Vincenty CA, Short AD, Alfonso A, Gill DL. A novel Ca2+ entry mechanism is turned on during growth arrest induced by Ca2+ pool depletion. J Biol Chem. 1995; 270:26790–26793. [PubMed: 7592918]
61. Miao YL, Stein P, Jefferson WN, Padilla-Banks E, Williams CJ. Calcium influx-mediated signaling is required for complete mouse egg activation. Proc Natl Acad Sci U S A. 2012; 109:4169–4174. [PubMed: 22371584]
62. Huang S, Maher VM, McCormick JJ. Extracellular Ca2+ stimulates the activation of mitogen-activated protein kinase and cell growth in human fibroblasts. Biochem J. 1995; 310 (Pt 3):881–885. [PubMed: 7575422]
63. Chen BB, Mallampalli RK. Masking of a nuclear signal motif by monoubiquitination leads to mislocalization and degradation of the regulatory enzyme cytidylyltransferase. Mol Cell Biol. 2009; 29:3062–3075. [PubMed: 19332566]

64. Huang S, Maher VM, McCormick J. Involvement of intermediary metabolites in the pathway of extracellular Ca2+-induced mitogen-activated protein kinase activation in human fibroblasts. Cell Signal. 1999; 11:263–274. [PubMed: 10372804]

65. Yoshida J, Ishibashi T, Nishio M. G1 cell cycle arrest by amlodipine, a dihydropyridine Ca2+ channel blocker, in human epidermoid carcinoma A431 cells. Biochem Pharmacol. 2007; 73:943–953. [PubMed: 17217918]

66. Takuwa N, Zhou W, Takuwa Y. Calcium, calmodulin and cell cycle progression. Cell Signal. 1995; 7:93–104. [PubMed: 7794690]

67. Berridge MJ, Lipp P, Bootman MD. The versatility and universality of calcium signalling. Nat Rev Mol Cell Biol. 2000; 1:11–21. [PubMed: 11413485]

68. Wayman GA, Tokumitsu H, Davare MA, Soderling TR. Analysis of CaM-kinase signaling in cells. Cell Calcium. 2011; 50:1–8. [PubMed: 21529938]

69. Kawanabe Y, Hashimoto N, Masaki T. Effects of extracellular Ca2+ influx on endothelin-1-induced intracellular mitogenic cascades in C6 glioma cells. Eur J Pharmacol. 2002; 435:119–123. [PubMed: 11821017]

70. Jensen TE, Rose AJ, Jorgensen SB, Brandt N, Schjerling P, et al. Possible CaMKK-dependent regulation of AMPK phosphorylation and glucose uptake at the onset of mild tetanic skeletal muscle contraction. Am J Physiol Endocrinol Metab. 2007; 292:E1308–1317. [PubMed: 17213473]

71. Wang P, Jiang Y, Wang Y, Shyy JY, DeFea KA. Beta-arrestin inhibits CAMKKbeta-dependent AMPK activation downstream of protease-activated-receptor-2. BMC Biochem. 2010; 11:36. [PubMed: 20858278]

72. Gormand A, Henriksson E, Strom K, Jensen TE, Sakamoto K, et al. Regulation of AMP-activated protein kinase by LKB1 and CaMKK in adipocytes. J Cell Biochem. 2011; 112:1364–1375. [PubMed: 21312243]

73. Chen BC, Wu WT, Ho FM, Lin WW. Inhibition of interleukin-1beta -induced NF-kappa B activation by calcium/calmodulin-dependent protein kinase kinase occurs through Akt activation associated with interleukin-1 receptor-associated kinase phosphorylation and uncoupling of MyD88. J Biol Chem. 2002; 277:24169–24179. [PubMed: 11976320]

74. Davare MA, Saneyoshi T, Guire ES, Nygaard SC, Soderling TR. Inhibition of calcium/calmodulin-dependent protein kinase kinase by protein 14-3-3. J Biol Chem. 2004; 279:52191–52199. [PubMed: 15469938]

Highlights

- We discover that Fbxl12 mediates CaMKI degradation via a proteasome-directed pathway
- We reveal a new CaMKI substrate, $p27^{Kip1}$
- We demonstrate that CaMKI regulates G1 progression via $p27^{Kip1}$ phosphorylation
- p27 phosphorylation by CaMKI is upstream to its phosphorylation by other kinases
- Increase of Fbxl12 expression induces G1 arrest via CaMKI degradation

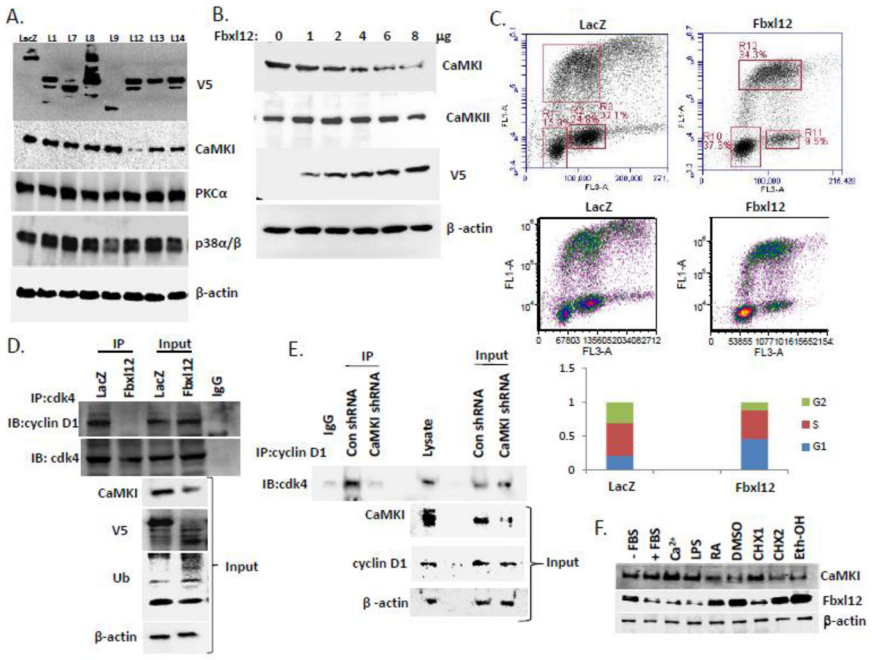

Figure 1. Ectopic expression of Fbxl12 disrupts the cdk4/cyclin D1 complex by mediating CaMKI degradation

(A) MLE cells were transfected with control plasmid *LacZ* or V5-tagged F-box proteins belonging to the L family. Cells were lysed and analyzed by immunoblotting using V5, CaMKI, PKCα, p38α/β and β-actin antibodies. (B) MLE cells transfected with increasing amounts of *Fbxl12* plasmid were analyzed by immunoblotting with CaMKI, CaMKII, V5 and β-actin antibodies. (C) Flow cytometric analysis of the cells transfected with *LacZ* and *Fbxl12* plasmids. (D) MLE cells transfected with control plasmid *LacZ* and *Fbxl12* plasmid were processed for immunoprecipitation using cdk4 antibody. The cdk4/cyclin D1 complex was then analyzed by immunoblotting using cyclin D1 antibody. (E) MLE cells were transfected with control shRNA and *CaMKI* shRNA. Cells were then collected followed by immunoprecipitation with cyclin D1 antibody and analyzed by immunoblotting with cdk4 antibody. (F) MLE cells were exposed to inducers of G1 arrest for 24 hours: LPS (100ng), RA (10 mM), 2% DMSO, CHX (1-0.5mg/ml, 2–2 mg/ml), and ethanol (100 mM). Cells were then harvested and processed for immunoblot analysis with Fbxl12 and CaMKI antibodies using β-actin as a control. The data from each panel represents n=3 separate experiments.

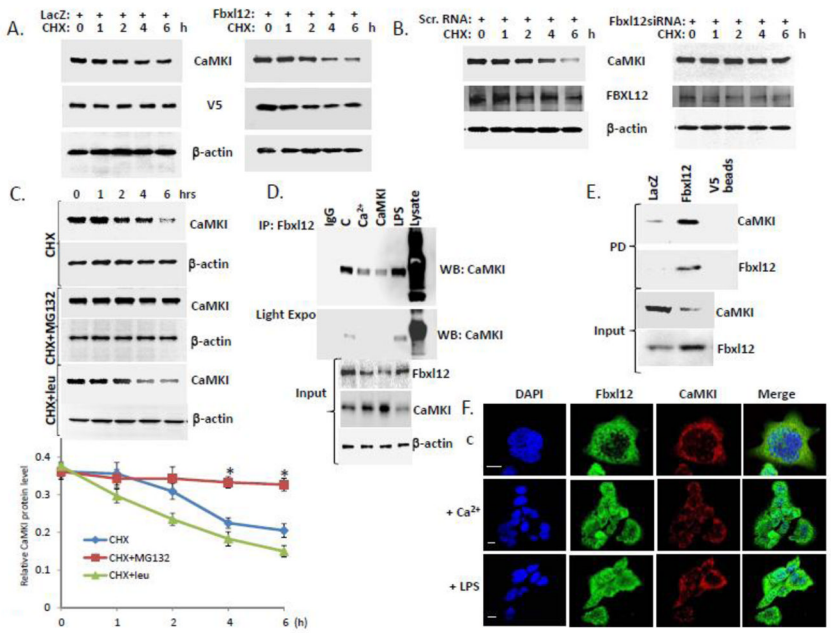

Figure 2. Fbxl12 binds CaMKI to trigger its degradation

(A–B) CaMKI half-life was determined after *Fbxl12* plasmid overexpression (A) or knockdown using scramble (scr) RNA or *Fbxl12* siRNA and cycloheximide (CHX) (B). (C) Levels of CaMKI in MLE cells exposed to MG132 and leupeptin in combination with cyclohexamide. Bottom graph shows quantification of CaMKI levels. (D) Immunoprecipitation using Fbxl12 antibody from MLE lysates after cells were exposed to Ca^{2+} or LPS or cells transfected with *CaMKI* plasmid; (C=control). Immunoprecipitants were analyzed by immunoblotting using CaMKI antibody. (E) MLE cells were transfected with *V5-LacZ* or *V5-Fbxl12* plasmids followed by pull down (PD) assays using V5 agarose beads and immunoblotting with CaMKI and Fbxl12 antibodies. (F) Cells exposed to Ca^{2+}or LPS were immunostained for Fbxl12 and CaMKI to determine subcellular localization. The data from each panel represents n=3 separate experiments. *P < .01 versus CHX treatment. Scale bar, 10 μm.

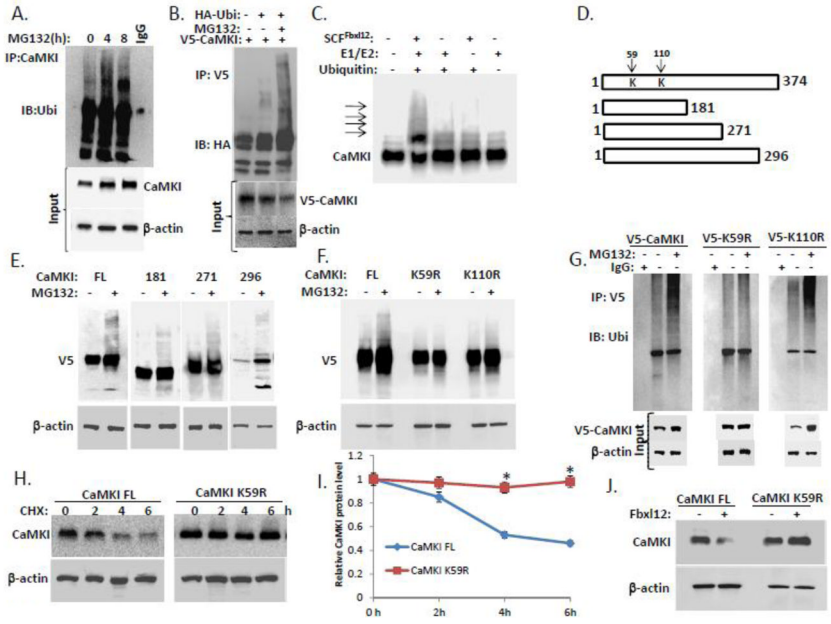

Figure 3. Fbxl12 targets CaMKI for ubiquitination

(A) *In vivo* ubiquitination assays. Ubiquitinated CaMKI was detected by immunoprecipitation of endogenous CaMKI followed by immunoblotting for ubiquitin after exposing cells to MG132. (B) MLE cells were transfected with V5-tagged CaMKI alone or co-transfected with HA-ubiquitin followed by MG132 exposure. Cells were then lysed and ubiquitinated V5-CaMKI was detected by immunoprecipitation with V5 antibodies followed by immunoblotting for HA antibodies. (C) *In vitro* ubiquitination assays. Purified SCF complex components were incubated with V5-CaMKI. The arrows show poliubiquitinated CaMKI. (D) Diagram of CaMKI deletion mutants. Arrows indicate putative ubiquitin acceptor sites. (E) Immunoblot analysis of cells transfected with V5-*CaMKI FL* or truncated V5-tagged *CaMKI* mutant plasmids followed by exposure to MG132. (F) Immunoblot analysis of cells transfected with V5-*CaMKI FL* or V5-tagged *CaMKI* point mutant plasmids (K59R and K110R) followed by exposure to MG132. (G) Cells transfected with V5-tagged (V5-*CaMKI FL*) or V5-tagged *CaMKI* point mutant plasmids (V5-K59R and V5-K110R) were exposed to MG132 and then processed for immunoprecipitation using V5 antibodies followed by immunoblotting with anti-ubiquitin antibodies. (H) Determination of CaMKI half-life using cycloheximide in cells expressing either *CaMKI FL* or the *CaMKI K59R* mutant plasmids with quantification (I). (J) Levels of CaMKI in the cells co-transfected with *CaMKI FL* or *CaMKI K59R* mutant plasmids after ectopic expression of *Fbxl12* plasmid (data are from n=3 experiments). *P < .01 versus CHX-treated *CaMKI FL*.

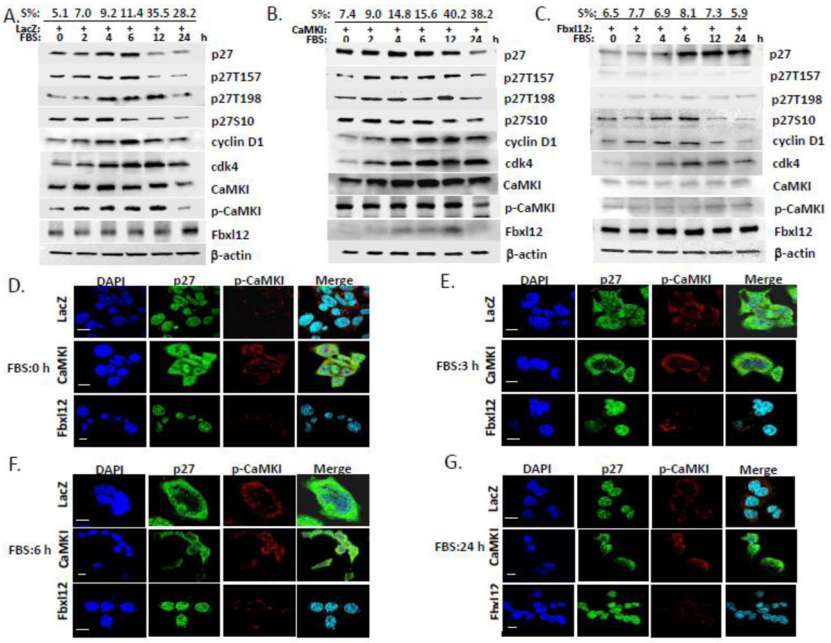

Figure 4. CaMKI controls cell cycle progression in lung epithelia via p27 phosphorylation and its subcellular localization

A549 cells were transfected with *LacZ* (A), *CaMKI* (B) or *Fbxl12*(C) plasmids followed by arrest at G0 by starvation. In 48 h 10% FBS was added and cells were collected at indicated times for flow cytometry and immunoblot analysis. The percentage of cells that entered into the S phase of the cell cycle are indicated at the top (S%). (D–G) CaMKI regulates p27 localization. MLE cells transfected with *LacZ, CaMKI* or *Fbxl12* as described above were fixed and processed for immunostaining using p-CaMKI and p27 antibodies at indicated times. DAPI was used to visualize the nucleus. Scale bar, 10 μm. The data from each panel represents at least n=3 separate experiments.

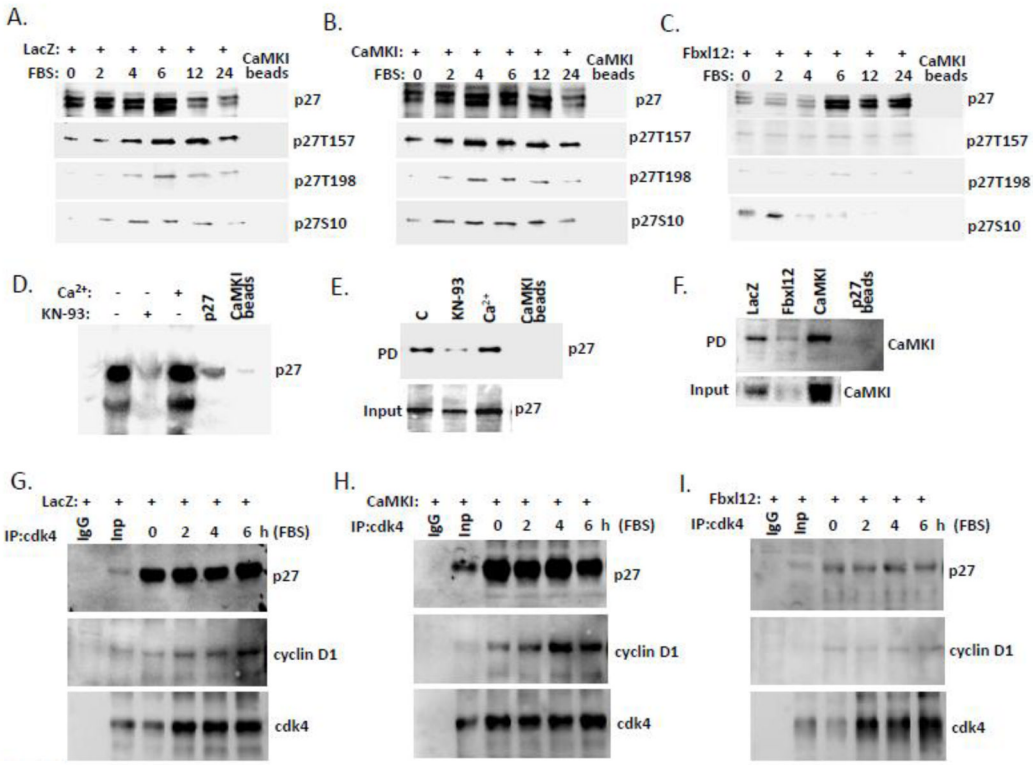

Figure 5. CaMKI binds p27 and regulates cdk4/cyclinD1/p27 complex formation

CaMKI binds p27. (A–C) A549 cells transfected with LacZ (A), CaMKI (B) and Fbxl12 (C) were starved for 48 hours and then recovered with addition of 10% FBS. Cells were then collected and processed for pull down assays using CaMKI-conjugated beads followed by immunoblotting with appropriate antibodies. (D) Direct binding between CaMKI and p27. Purified recombinant p27 was pre-incubated with CaMKI beads with or without Ca^{2+} or KN-93 as indicated on top of the lanes, followed by immunoblot analysis with p27 antibody. (E) Cells exposed to KN-93 (20μM) or Ca^{2+}(2mM) for 1 h were then collected followed by pull down assays using CaMKI-conjugated beads. (F) Cells transfected as described above (A–C) were processed for pull down assays using beads conjugated to p27 followed by immunoblot analysis with CaMKI antibody. (G–I) CaMKI regulates cdk4/cyclinD1/p27 complex formation. Cells transfected with *LacZ* (G), *CaMKI* (H) or *Fbxl12* plasmids (I) were released with 10% FBS addition and then collected at indicated times for immunoprecipitation using cdk4 antibody. Immunoprecipitants and input were analyzed by imuunoblotting using p27 and cyclin D1 antibodies. n=2 experiments.

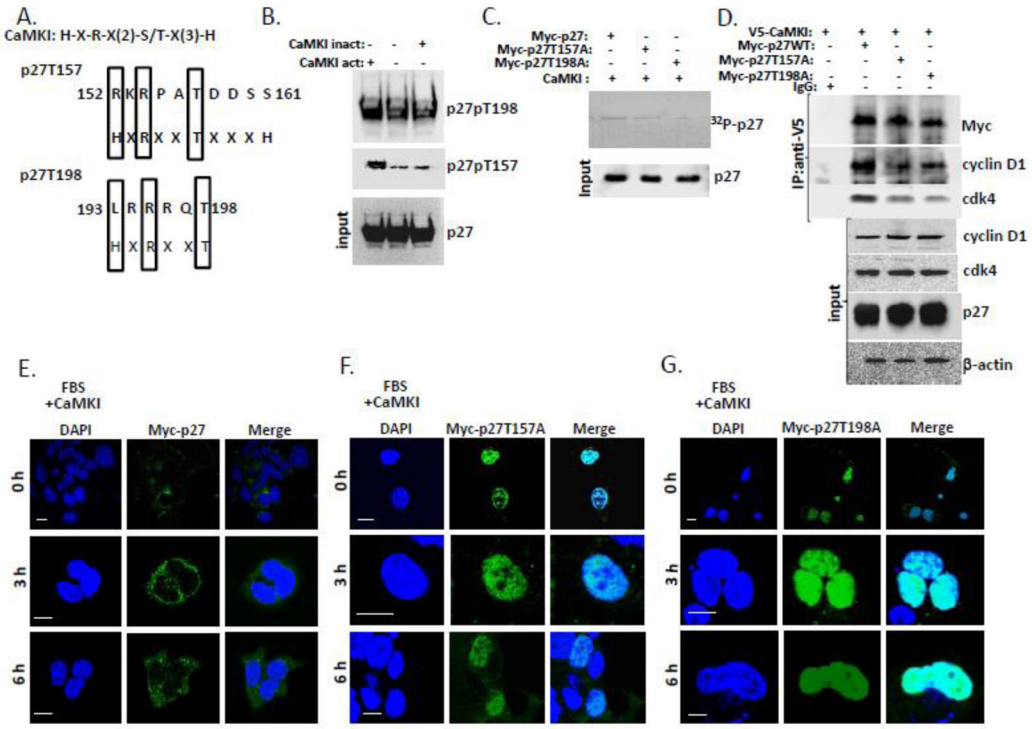

Figure 6. CaMKI phosphorylates human p27 and regulates its intracellular localization in human lung epithelia

(A) Alignment of the CaMKI consensus recognition motif and putative phosphorylation sites within human p27. (B) Purified CaMKI phosphorylates recombinant human p27 at T157 and T198 *in vitro*. p27 (3μg) was incubated with 10 μCi [γ-^{32}P]ATP in the presence or absence of the active form of CaMKI (500 nM) and heat-inactivated CaMKI form. After 1 h of incubation at 30°, reactions were terminated with 4X Laemmli protein loading buffer and products were resolved by 10% SDS-PAGE and analyzed by immunoblotting using antibodies against total and phospho-specific forms of p27 (p27, T157 and T198). (C) CaMKI phosphorylates p27 WT but not p27 mutants in human lung epithelia. A549 cells were transfected with *Myc-tagged p27 WT* or p27 point mutants *p27 T157A* or *p27 T198A.* Myc-tagged proteins were then pulled down with Myc-agarose. The Myc-p27-, Myc-p27T157A- and Myc-p27T198A- beads were first dephosphorylated using alkaline phosphatase (5 U) followed by incubation with the active form of CaMKI (500nM) in the presence of 10 μCi [γ-^{32}P]ATP and Ca^{2+} (2 mM). After 1 h of incubation at 30°, reaction products were resolved by 10% SDS-PAGE and analyzed by autoradiography and immunoblotting. (D) CaMKI induces binding of cdk4 and cyclin D1 with wild type of p27 but not with the p27 point mutants. A549 cells were co-transfected with *V5-CaMKI* and either *Myc-p27*, *Myc-p27 T157A* or *Myc-p27 T198A* plasmids followed by immunoprecipitation with V5 antibody. Immunoprecipitants and input were analyzed by immunoblotting using an appropriate antibody. (E–G) A549 cells were co-transfected with *CaMKI* and either *Myc-p27 (E), Myc-p27T157A (F) or Myc-p27T198A* plasmids (G). Cells were then synchronized by serum starvation and released in 48 h by addition of 10% FBS followed by fixation at indicated times and immunostaining using anti-Myc antibody and DAPI to visualize nuclei. The data from each panel represents at least n=3 separate experiments. Scale bar, 10 μm.

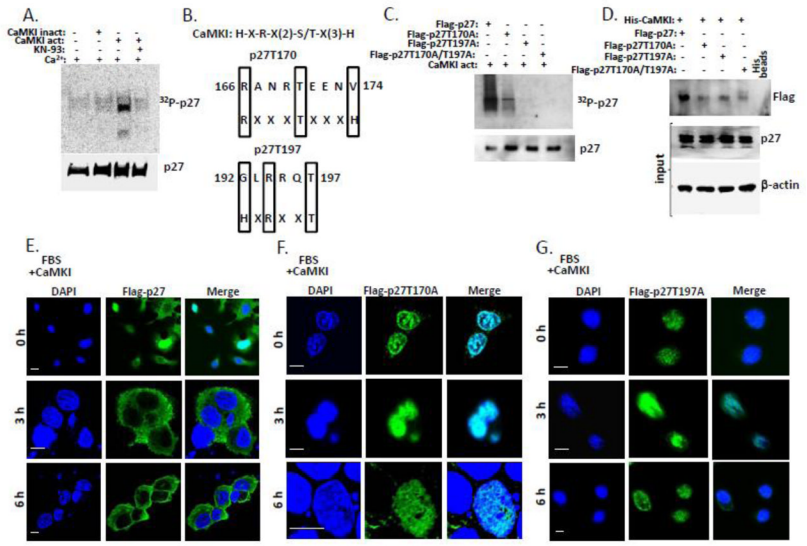

Figure 7. CaMKI phosphorylates mouse p27 and regulates its intracellular localization in mouse lung epithelium

(A) Purified CaMKI phosphorylates p27 purified from mouse cells *in vitro*. Purified p27 from MLE cells was incubated with 10 μCi [γ-^{32}P]ATP in the presence or absence of an active or heat-inactivated form of CaMKI (500 nM) and Ca^{2+}. After 1 h of incubation with or without KN-93 at 30°, reactions were terminated with 4X Laemmli protein loading buffer and products were resolved by 10% SDS-PAGE and analyzed by autoradiography and immunoblotting using p27 antibodies. (B) Alignment of the CaMKI consensus recognition sequence and putative phosphorylation sites within mouse p27. (C) CaMKI phosphorylates p27 WT but not mutants in mouse lung epithelia. MLE cells were transfected with *Flag-tagged p27 WT* or mutants *p27T170A, p27T197A* or *p27T170A / T197A*. Flag-tagged proteins were then pulled down with Flag-agarose. The Flag-p27-, Flag-p27T157A-, Flag-p27T198A- and Flag p27T170A / T197A -beads were dephosphorylated using alkaline phosphatase and then incubated with 10 μCi [γ-^{32}P]ATP in the presence of an active form of CaMKI (500 nM) and Ca^{2+} (2 mM). After 1 h of incubation at 30°, reaction products were resolved by 10% SDS-PAGE and analyzed by autoradiography and immunoblotting. (D) CaMKI associates with p27 wild type but not with point mutants. MLE cells were co-transfected with *His-CaMKI* and either *Flag-p27, Flag-p27T157A, Flag-p27T198A* or *Flag-p27T170A / T197A* plasmids followed by pull down with His-conjugated beads. Samples were then analyzed by immunoblotting using protein specific antibodies. (E–G) MLE cells were co-transfected with *CaMKI* and either *Flag-p27 (E), Flag-p27T170A (F) or Flag-p27T197A* plasmids (G). Cells were then synchronized by serum starvation and released in 48 h by addition of 10% FBS followed by fixation at indicated times and immunostaining using anti-Flag antibody and DAPI to visualize nuclei. The data are from n=3 experiments. Scale bar, 10 μm.

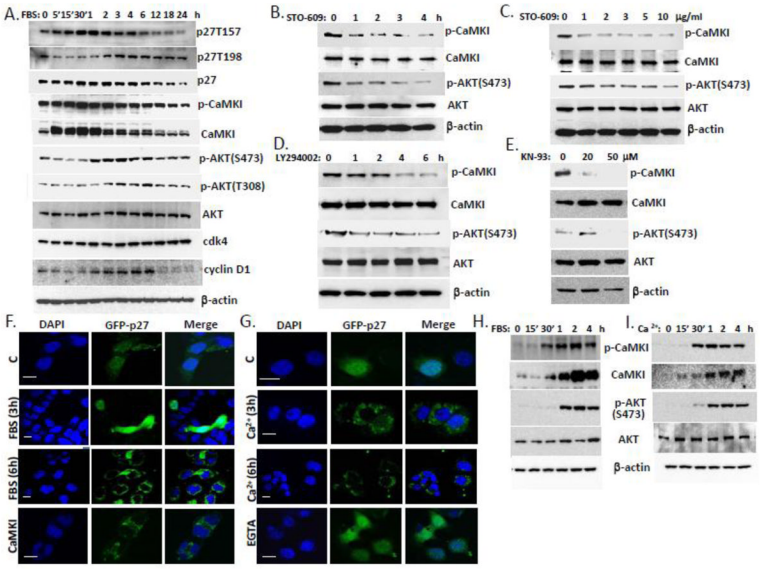

Figure 8. Coordinate regulation of CaMKI and AKT activities via Ca^{2+} and serum control p27 localization in lung epithelia

(A) A549 cells were synchronized by serum starvation for 48 h. After 10% FBS addition cells were collected at indicated times and processed for immunoblotting for proteins of interest. (B, C) MLE cells were exposed to the CaMKK inhibitor, STO-609 (10 μg/ml) at various times (B) and concentrations (C, 2 h). (D, E) Cells were also exposed to the AKT inhibitor, LY294002 (30 μM) at various time (D) or CaMKI inhibitor, KN-93 for 1 h (E) and then analyzed by immunoblotting using antibodies against CaMKI, AKT, and phosphorylation forms. (F,G) MLE cells transfected with GFP-p27 were starved by serum depletion for 48 h and then exposed to 10% FBS (A) or 2 mM Ca^{2+} (B) followed by fixation at indicated times and immunostaining. Some of these cells were pre-incubated with EGTA as described above or co-transfected with *CaMKI* plasmid. DAPI was used for visualization of nuclei. Scale bar, 10 μm. (H,I) MLE cells were synchronized by starvation for 48 h and then exposed to 10% FBS (H) or 2 mM Ca^{2+} (I) for indicated times. Cells were then harvested and analyzed by immunoblotting with CaMKI and AKT antibodies (data are from n=3 experiments).